

Decay of $^{90}\text{Rb}^g$ and $^{90}\text{Rb}^m$

W. L. Talbert, Jr.

*Ames Laboratory-DOE and Department of Physics, Iowa State University, Ames, Iowa 50011
and University of California, Los Alamos Scientific Laboratory, Los Alamos, New Mexico 87545**F. K. Wahn and L. J. Alquist[†]*Ames Laboratory-DOE and Department of Physics, Iowa State University, Ames, Iowa 50011*

C. L. Duke

Physics Department, Grinnell College, Grinnell, Iowa 50112

(Received 12 November 1980)

The β and subsequent γ decays of $^{90}\text{Rb}^g$ and $^{90}\text{Rb}^m$ have been studied using an on-line isotope separator system. Ge(Li) γ -ray singles and γ - γ coincidence measurements were used to construct level schemes for ^{90}Sr . The decays of the two ^{90}Rb activities were distinguished using a set of four experiments in which the collection and observation parameters were adjusted to change the relative decay intensities. For the decay of $^{90}\text{Rb}^g$, 83 attributed γ -ray transitions were placed among 33 excited states of ^{90}Sr , whereas for the decay of $^{90}\text{Rb}^m$, 43 excited states of ^{90}Sr provided placement for 108 attributed γ rays. Twelve γ rays were not placed in either level scheme, and 42 transitions are common to both decays. Spin and parity assignments have been deduced using γ -decay $\log ft$ values, γ - γ angular correlation data, and reaction data in the literature. Interpretation of some of the energy levels is made from a shell-model viewpoint.

[RADIOACTIVITY $^{90}\text{Rb}^g$, $^{90}\text{Rb}^m$ [decay products of ^{90}Kr from $^{235}\text{U}(n, f)$]; measured E_γ , I_γ , γ - γ^{coin} , $\gamma\gamma^{(\theta)}$. Ge(Li) and NaI(Tl) detectors. ^{90}Sr deduced levels, J , π , $\log ft$. Mass-separated ^{90}Kr activity.]

I. INTRODUCTION

The study of the decays $^{90}\text{Rb}^g$ and $^{90}\text{Rb}^m$ has been in progress at the TRISTAN on-line isotope separator facility.¹ These decays are of interest because of the proximity of the daughter nucleus to the subshell and shell closures at $Z=38$ and $N=50$. The two decay modes of ^{90}Rb offer an unusual opportunity to observe different sets of levels in ^{90}Sr populated directly in β decay, but impose experimental difficulties in the separation of the two decays. The ^{90}Rb decays were studied as decay products of mass-separated ^{90}Kr . The decay of ^{90}Kr was reported earlier.² This study reports results that have appeared in Nuclear Data Sheets in preliminary form.³ Several important changes or additions to the preliminary results have developed subsequently, the most important being the successful separation of the ground-state and isomeric-state decays of ^{90}Rb . In addition, new spin information for the decaying states of ^{90}Rb is available from measurements at the ISOLDE facility at CERN.⁴ Although an exhaustive literature survey of prior decay studies would be too lengthy for presentation here because of the rich history of such studies over the years, a few selected references follow to place the present work in perspective.

The first comprehensive study of ^{90}Rb using

high-resolution detectors was published by Mason and Johns.⁵ In that report, very preliminary results from the present work were included. Our work has modified the decay schemes of Mason and Johns in a number of important respects, especially in the more complete separation of the isomeric and ground-state decay transitions. Earlier work was adequately summarized by Mason and Johns, including the history surrounding the establishment of the two β -decay modes of ^{90}Rb . Singh and Johns⁶ reported the first directional correlation measurements for transitions from the decay of ^{90}Rb . The angular correlation data reported here expand considerably the earlier results.

Decay parameters adopted in Nuclear Data Sheets are $T_{1/2}(^{90}\text{Rb}^g) = 153 \pm 3$ s,⁷ $T_{1/2}(^{90}\text{Rb}^m) = 258 \pm 5$ s,⁸ and $Q_\beta(^{90}\text{Rb}^g) = 6360 \pm 60$ keV.⁹ Direct measurements at the TRISTAN facility of the last two quantities are $T_{1/2}(^{90}\text{Rb}^m) = 251 \pm 10$ s (Ref. 7) and $Q_\beta(^{90}\text{Rb}^g) = 6550 \pm 60$ keV.¹⁰ The latter value is used for $\log ft$ calculations in this work and is consistent with the most recently reported value of 6578 ± 15 keV.¹¹

After the work of Mason and Johns, and in addition to the present work, γ -ray measurements for the decays of ^{90}Rb were reported by the Orsay and McGill groups,^{12,13} in which the Rb fission products were mass separated directly (and

apparently contained a higher portion of the isomeric decay¹⁴ than is observed from the decay of ^{90}Kr . The study by Huang *et al.*¹³ is quite complete, but, as will be pointed out later, there are significant differences from the present results.

Recently, Ekström *et al.* measured the spins of the ^{90}Rb isomers.⁴ This information has been adopted in the discussion of the ^{90}Rb decays and departs from the spins previously assumed (the ground-state and isomer spins are reported to be 0 and 3, respectively, rather than 1 and 4 as previously assumed).

The structure of ^{90}Sr has been probed using the $^{88}\text{Sr}(t, p)$ reaction in a study that also reviews nicely the systematics of pairing states near $N=50$.¹⁵ As will be discussed later, the results of this work are in substantial agreement with the reaction data (where levels are seen in both studies), with a few notable exceptions.

II. EXPERIMENTAL TECHNIQUES

A. Sample preparation

The ^{90}Rb activities were produced from decay of ^{90}Kr obtained from thermal neutron fission of ^{235}U , followed by on-line mass separation with the TRISTAN facility at the Ames Laboratory research reactor. At the time of these measurements, the ^{235}U target was connected to the oscillating electron ion source of the mass separator by a room-temperature 1.6-m-long transport line; thus, only gaseous fission products could reach the ion source. Because the facility has been described in detail previously,¹ only a few pertinent features need to be mentioned.

The $A=90$ samples obtained in the present study had less than two parts in 10^5 of contaminating activities from neighboring masses. Some of the samples, however, contained non-negligible amounts of ^{89}Kr arising from Kr hydride molecular ions present in the mass-separated beam.¹ The resulting presence of ^{89}Kr and ^{89}Rb activities was not serious, however, because these activities have been well measured.¹⁶ Furthermore, the ion source produced much fewer hydride molecular ions than Kr^+ , and the $A=89$ activities were only small fractions of the total activity at $A=90$.

Because the ^{90}Rb activities arose from the decay of even-even ^{90}Kr , the low-spin $^{90}\text{Rb}^g$ decay was preferentially observed. Thus, this work serves to complement that of Huang *et al.*,¹³ where the ^{90}Rb activities were obtained directly from fission (with a preponderance of $^{90}\text{Rb}^m$ activity). The high-activity yield of ^{90}Kr in the TRISTAN facility allowed the flexible use of the moving tape collector¹ to provide sources ranging

from equilibrium with the ^{90}Kr activity to nearly pure isomer decays. For this work, four different modes of the moving tape collector were used to effect a clean distinction between the $^{90}\text{Rb}^g$ and $^{90}\text{Rb}^m$ decay transitions. Compared to an equilibrium decay from ^{90}Kr , the other moving tape collector parameters yielded isomer-to-ground-state activity ratios of 1.65, 1.96, and 11.5. The data reported in Nuclear Data Sheets³ have the ratio of 1.65, and the spectra were not analyzed at that time for distinguishing isomer from ground-state decay transitions. From these four sets of data, the isomer and ground-state decay transitions can be determined with reasonable certainty. In some cases, the assignment of transitions to $^{90}\text{Rb}^g$ or $^{90}\text{Rb}^m$ disagrees with that of Huang *et al.*, but there is general agreement.

B. γ -ray measurements

γ -ray singles and coincidence data were obtained from two Ge (Li) detectors having approximately 10% relative efficiency and 2.5-keV resolution (at 1332 keV). The two-parameter coincidence studies used a 4096×4096 format, 180° detector orientation, and 40-ns coincidence timing window. Approximately 3×10^6 coincidence events were recorded. In scanning the coincidence data, 82 gates were used, considerably more than the 32 gates used in the study by Huang *et al.*¹³ All singles spectra were analyzed using standard computer-based methods, and the gated spectra were analyzed both visually and by computer fitting techniques.

C. γ - γ angular correlation measurements

The angular-correlation apparatus in this study has been described elsewhere.^{17,18} The apparatus consists of six NaI(Tl) detectors positioned at specific angles of 45° , 90° , 135° , 180° , 225° , and 292.5° relative to one Ge(Li) detector. Simultaneous γ - γ coincidences were established between the six Ge(Li)-NaI(Tl) pairs by virtue of six independent fast-coincidence circuits. Energy pulses from each NaI(Tl) detector were selected by the energy window setting in a corresponding single-channel analyzer, set in this study to trigger on the first-excited-to-ground-state transition at 831 keV, presumed to be a pure $E2$, $2^+ \rightarrow 0^+$ transition. The source strength was monitored throughout the experiment and was held below $7 \mu\text{Ci}$ so that the accidental-to-true-coincidences ratio was less than 2%. Thus, accidentals corrections were unnecessary. The Ge(Li) spectra at various pair angles were analyzed for the transitions of interest, and the angular correlation data were fitted to the form $W(\theta) = 1$

$+A_2P_2(\cos\theta)+A_4P_4(\cos\theta)$. The errors in A_2 and A_4 were determined as discussed elsewhere.^{17,18} The mixing ratio δ for mixed transitions was defined in accordance with the sign convention of Taylor *et al.*¹⁹

III. EXPERIMENTAL RESULTS

A. γ -ray measurements

The γ -ray spectrum for ^{90}Rb -enhanced decay is shown in Fig. 1. The contributions to this spectrum from ^{89}Kr are quite small, and the enhancement over the ^{90}Kr decay spectrum is substantial. For the moving tape collector conditions of this measurement (900-s collect time, 150-s delay time, and 750-s count time), the isomer activity was enhanced by a factor of 1.65 relative to the equilibrium data. The separation of isomer and ground-state transitions is illustrated in Fig. 2, where the 1793.89-keV isomer-decay transition is compared to the 1804.10-keV ground-state-decay transition for the conditions of equilibrium, intermediate, and isomer-enhanced moving tape-collector parameters. Clear distinction could be made for γ -ray attribution in most of the intense transitions. During the construction of the decay schemes, these clear attributions could be used to confirm attributions indicated for the weaker transitions depopulating the same excited levels. The resulting list of observed γ -ray transitions is shown in Table I, where intensities have been assigned for either/both decays as observed.

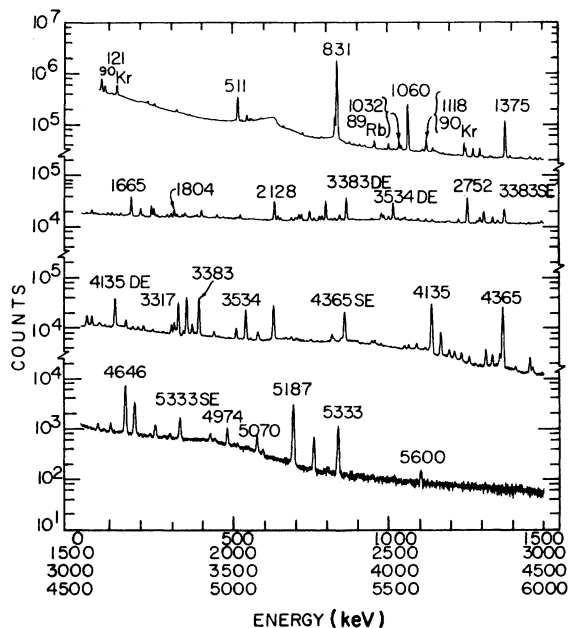


FIG. 1. ^{90}Rb -enhanced γ -ray spectrum, taken at an isomer-to-ground-state activity ratio of 1.65.

In comparing the results of this work with those of Huang *et al.*,¹³ the following differences are noted: Huang *et al.* observe 114 γ -ray transitions, whereas 161 γ rays are listed here. Of the ten γ rays reported by Huang *et al.* not listed here, six were not placed in a decay scheme, and one is attributed in this work as a contaminant. The attribution of only six transitions is different between the two studies, but it should be noted that only one of these six is placed in a level scheme in Ref. 13, whereas five are placed in this work. The γ -ray doublets at 825 and 1892 keV reported by Huang *et al.* were not observed in this work. Because of the more complete decay schemes we are presenting, 24 transitions are present in both decays that were assigned only to one decay in Ref. 13. The 4061-, 4332-, 4454-, and 4599-keV transitions clearly seen in the 831-keV coincidence spectrum in Ref. 13 were not observed clearly in the coincidence studies

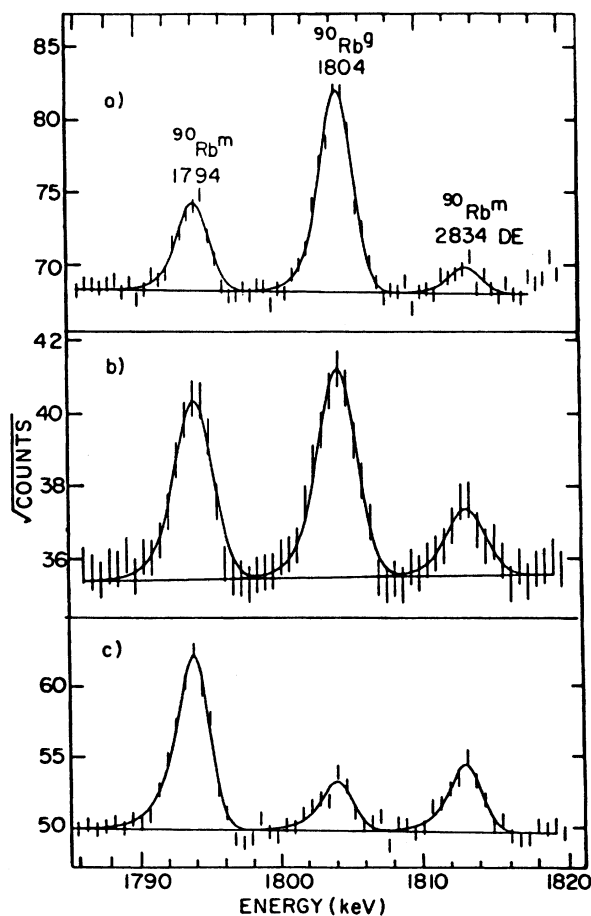


FIG. 2. Segment of γ -ray spectrum, showing relative transition strengths for (a) equilibrium, (b) isomer-to-ground-state ratio of 1.96, and (c) isomer-to-ground-state ratio of 11.5.

TABLE I. Photopeaks observed in the decays of $^{90}\text{Rb}^f$ and $^{90}\text{Rb}^m$.

Energy (keV)	Intensity for ground-state decay ^a	Intensity for isomer decay ^a	Placement (keV)
106.92 ± 0.15		2.3 ± 0.3	Isomeric transition
196.8 ± 0.4	2.4 ± 0.4		5623 → 5426
314.5 ± 0.3	0.22 ± 0.02	8.8 ± 0.4	2207 → 1892
395.8 ± 0.8		0.8 ± 0.4	5822 → 5426
442.3 ± 0.4		1.2 ± 0.3	4808 → 4366
552.10 ± 0.13		4.2 ± 0.3	3449 → 2927
543.6 ± 1.0	1.6 ± 0.7		4580 → 4037
551.20 ± 0.25	0.23 ± 0.03	9.1 ± 0.7	2207 → 1655
720.70 ± 0.09	0.34 ± 0.03	5.7 ± 0.4	2927 → 2207
739.2 ± 0.4	1.26 ± 0.22	w	4366 → 3627
752.1 ± 0.3	1.77 ± 0.22	w	4135 → 3383
765.1 ± 0.7	0.04 ± 0.02	0.9 ± 0.3	4148 → 3383
779.9 ± 0.4		2.9 ± 0.6	4335 → 3555
824.23 ± 0.10	5.2 ± 0.4	92 ± 5	1655 → 831
831.69 ± 0.05	1000 ± 37	1000 ± 38	831 → 0
872.00 ± 0.15		5.6 ± 0.4	2527 → 1655
886.3 ± 0.3	1.6 ± 0.3	w	3383 → 2497
892.5 ± 0.7	0.7 ± 0.3		4037 → 3144
921.20 ± 0.24		3.2 ± 0.7	3449 → 2527
952.44 ± 0.07		17.9 ± 0.6	3449 → 2497
985.4 ± 0.5	0.59 ± 0.18	0.85 ± 0.25	3555 → 2570
997.85 ± 0.06	11.4 ± 0.4		4037 → 3039
1003.9 ± 0.9	w	0.6 ± 0.3	4148 → 3144
1013.95 ± 0.19		2.7 ± 0.3	3584 → 2570
1021.9 ± 0.7		0.8 ± 0.3	4404 → 3383
1027.1 ± 0.4	0.50 ± 0.07	1.3 ± 0.3	3954 → 2927
1038.63 ± 0.07	7.8 ± 0.3		5187 → 4148
1060.70 ± 0.04	239 ± 8	81 ± 3	1892 → 831
1086.7 ± 0.8		0.74 ± 0.15	3584 → 2497
1109.2 ± 0.8		1.4 ± 0.8	4036 → 2927
1140.50 ± 0.06	1.63 ± 0.10	9.4 ± 0.5	3032 → 1892
1146.96 ± 0.25	1.07 ± 0.13	0.16 ± 0.05	3039 → 1892
1176.9 ± 0.9	1.0 ± 0.4	w	3383 → 2207
1242.84 ± 0.04		32.2 ± 1.8	3449 → 2207
1271.77 ± 0.07	0.98 ± 0.06	16.4 ± 2.2	2927 → 1655
1298.5 ± 0.5		2.1 ± 0.4	4854 → 3555
1302.2 ± 0.3		2.0 ± 0.5	4685 → 3383
1326.46 ± 0.21	3.3 ± 0.4	w	4366 → 3039
1375.36 ± 0.03	4.5 ± 0.7	177 ± 7	2207 → 831
1377.2 ± 0.5		24 ± 8	3584 → 2207
1391.6 ± 0.3		4.6 ± 0.8	4430 → 3039
1425.2 ± 0.3		2.9 ± 0.3	4808 → 3383
1430.4 ± 0.4	1.26 ± 0.22 ^b		
1438.3 ± 0.8	0.8 ± 0.3	w	4366 → 2927
1456.7 ± 0.3	0.95 ± 0.09	2.5 ± 0.7	3954 → 2497
1460.1 ± 0.6		2.0 ± 0.5	4430 → 2971
1485.6 ± 0.7	1.7 ± 0.5		5041g → 3555
1489.0 ± 0.4	0.77 ± 0.14	3.7 ± 0.5	3144 → 1655
1522.1 ± 0.4	0.96 ± 0.22		4019 → 2497
1547.8 ± 0.5	1.6 ± 0.4		4580 → 3032
1576.9 ± 0.7		1.2 ± 0.4	5026 → 3449
1590.3 ± 0.3	3.5 ± 0.4		4973 → 3883
1603.52 ± 0.20		4.9 ± 0.5	5557 → 3954
1631.78 ± 0.20	2.1 ± 0.4		5187 → 3555
1658.9 ± 0.3		4.6 ± 0.6	5285 → 3627
1665.61 ± 0.07	5.40 ± 0.22	51.0 ± 1.2	2497 → 831
1668.9 ± 0.6	3.8 ± 1.3		5623 → 3954

TABLE I. (Continued)

Energy (keV)	Intensity for ground-state decay ^a	Intensity for isomer decay ^a	Placement (keV)
1686.2 ± 0.6		1.3 ± 0.4	5822 → 4135
1692.07 ± 0.25		2.9 ± 0.5	3584 → 1892
1696.16 ± 0.07		17.5 ± 0.6	2527 → 831
1738.93 ± 0.08	0.58 ± 0.02	20.0 ± 0.8	2570 → 831
1747.3 ± 0.3	0.95 ± 0.11	2.5 ± 0.4	3954 → 2207
1764.5 ± 0.9		1.0 ± 0.5	4335 → 2570
1793.89 ± 0.11		8.9 ± 0.5	3449 → 1655
1804.10 ± 0.07	15.2 ± 0.5		5187 → 3383
1829.82 ± 0.20		3.7 ± 0.5	4036 → 2207
1838.15 ± 0.14		8.7 ± 0.6	4335 → 2497
1842.3 ± 0.5	0.6 ± 0.4		(2674 → 831) ^c
1870.7 ± 0.4	1.9 ± 0.4		5254 → 3383
1877.40 ± 0.21		4.7 ± 0.5	4805 → 2927
1892.28 ± 0.08	14.4 ± 0.6	4.9 ± 0.5	1892 → 0
1903.1 ± 0.6		1.4 ± 0.6	4430 → 2527
1941.81 ± 0.17	0.31 ± 0.03	6.5 ± 0.6	4148 → 2207
1973.3 ± 1.0	1.0 ± 0.4		5600 → 3627
1996.0 ± 1.0	1.0 ± 0.4		5623 → 3627
2119.7 ± 0.8	1.9 ± 0.7 ^b		
2128.30 ± 0.07		55.2 ± 1.5	4335 → 2207
2139.33 ± 0.18	11.1 ± 0.6	1.4 ± 0.6	2971 → 831
2148.2 ± 0.3	5.5 ± 0.7		5187 → 3039
2200.9 ± 0.3		5.1 ± 0.6	5828 → 3627
2207.47 ± 0.11	11.4 ± 0.5	1.71 ± 0.12	3039 → 831
2216.29 ± 0.14	12.5 ± 0.7		5187 → 2971
2239.7 ± 0.8	4.1 ± 2.2		5623 → 3383
2245.2 ± 0.9	1.6 ± 1.0		4137 → 1892
2256.55 ± 0.17	0.32 ± 0.02	7.0 ± 0.5	4148 → 1892
2298.1 ± 0.9	1.4 ± 0.6	3.6 ± 2.0	3954 → 1655
2311.2 ± 0.6		3.1 ± 1.0	4808 → 2497
2335.2 ± 1.0		2.2 ± 0.9	5785 → 3449
2381.5 ± 0.5		1.8 ± 0.7	4036 → 1655
2442.9 ± 0.5		2.8 ± 0.7	4335 → 1892
2473.94 ± 0.20	15.4 ± 1.5	0.09 ± 0.01	4366 → 1892
2476.7 ± 1.1	2.7 ± 1.7		4973 → 2497
2497.27 ± 0.15	0.85 ± 0.09	8.1 ± 0.8	2497 → 0
2537.8 ± 0.9		1.8 ± 0.7	4430 → 1892
2543.9 ± 0.3		3.5 ± 0.4	5041 _m → 2497
2592.32 ± 0.20		6.8 ± 0.7	5089 → 2497
2617.8 ± 0.3		6.5 ± 0.9	3449 → 831
2688.9 ± 0.5	3.1 ± 0.6		4580 → 1892
2724.26 ± 0.21	3.2 ± 0.4	4.6 ± 0.6	3555 → 831
2741.0 ± 1.2		1.5 ± 0.8	4947 → 2207
2752.68 ± 0.08		122 ± 4	3584 → 831
2789.1 ± 2.2		3.0 ± 1.9	5822 → 3032
2834.43 ± 0.13		19.6 ± 1.2	5041 _m → 2207
2900.3 ± 1.3		1.2 ± 0.7	5828 → 2927
2911.7 ± 1.1		1.3 ± 0.7	4804 → 1892
2924.3 ± 0.7	1.8 ± 0.6		4580 → 1655
2980.7 ± 0.6	2.4 ± 0.5		5187 → 2207
3032.1 ± 0.5		4.6 ± 0.7	5239 → 2207
3039.17 ± 0.12	18.7 ± 0.7	2.76 ± 0.21	3039 → 0
3081.3 ± 0.4	3.9 ± 0.7		4973 → 1892
3148.58 ± 0.12	10.5 ± 0.4		5041 _g → 1892
3197.9 ± 1.0		1.5 ± 0.6	4854 → 1655
3205.09 ± 0.16		11.9 ± 0.9	4036 → 831
3214.5 ± 1.1		1.4 ± 0.6	5785 → 2570
3295.09 ± 0.14	21.6 ± 1.0		5187 → 1892

TABLE I. (Continued)

Energy (keV)	Intensity for ground-state decay ^a	Intensity for isomer decay ^a	Placement (keV)
3303.91 ± 0.13	22.1 ± 0.9	0.15 ± 0.01	4135 → 831
3317.00 ± 0.12	7.12 ± 0.22	152 ± 4	4148 → 831
3361.88 ± 0.13	24.4 ± 1.0		5254 → 1892
3370.8 ± 0.4		4.2 ± 0.6	5026 → 1655
3383.24 ± 0.12	168 ± 5	6.52 ± 0.14	3383 → 0
3503.52 ± 0.15		25.1 ± 1.1	4335 → 831
3534.24 ± 0.13	101 ± 3	0.77 ± 0.03	5426 → 1892
3538.6 ± 0.6		5.1 ± 1.1	5431 → 1892
3572.82 ± 0.18		16.3 ± 1.0	4404 → 831
3620.8 ± 1.1		6.1 ± 2.3	5828 → 2207
3627.4 ± 0.7	3.2 ± 1.3	10 ± 4	3627 → 0
3664.0 ± 0.5	2.1 ± 0.4 ^b		
3814.36 ± 0.20	14.7 ± 1.0		4646 → 831
3929.4 ± 1.4		1.4 ± 0.8	5822 → 1892
3958.4 ± 0.8	2.0 ± 0.6		4790 → 831
3972.2 ± 0.5		3.8 ± 0.7	4804 → 831
4019.3 ± 1.3	0.9 ± 0.4		4019 → 0
4061.7 ± 0.3	6.0 ± 0.7 ^b		
4087.26 ± 0.23	6.4 ± 0.4		4919 → 831
4115.6 ± 0.4		3.7 ± 0.6	4947 → 831
4135.51 ± 0.17	168 ± 6	1.17 ± 0.04	4135 → 0
4192.75 ± 0.23		12.1 ± 1.1	5024 → 831
4209.5 ± 0.3		9.6 ± 0.9	5041 ^m → 831
4257.34 ± 0.24		7.8 ± 0.6	5089 → 831
4278.4 ± 0.8	1.3 ± 4 ^b		
4332.14 ± 0.20	9.9 ± 0.6 ^b		
4335.78 ± 0.22	11.1 ± 0.6		5187 → 831
4365.90 ± 0.18	200 ± 7	1.13 ± 0.08	4366 → 0
4454.07 ± 0.21		12.5 ± 0.8	5285 → 831
4500.8 ± 1.0	0.9 ± 0.4		5333 → 831
4599.4 ± 0.3		4.9 ± 0.4	5431 → 831
4635.1 ± 0.4	0.6 ± 0.3 ^b		
4646.45 ± 0.20	56.4 ± 2.2		4646 → 0
4685.0 ± 1.4		0.4 ± 0.3	4685 → 0
4726.1 ± 0.7		1.2 ± 0.3	5557 → 831
4790.2 ± 0.7	1.6 ± 0.4		4790 → 0
4919.0 ± 0.4	1.92 ± 0.22		4919 → 0
4934.8 ± 0.7	0.89 ± 0.22 ^b		
4974.14 ± 0.25	5.2 ± 0.4		4973 → 0
4996.12 ± 1.1		0.7 ± 0.3	5828 → 831
5007.7 ± 0.9	0.59 ± 0.22 ^b		
5070.2 ± 0.3	3.6 ± 0.3 ^b		
5187.44 ± 0.23	29.2 ± 1.2		5187 → 0
5254.27 ± 0.25	5.8 ± 0.4		5254 → 0
5299.5 ± 0.9	0.43 ± 0.14 ^b		
5333.01 ± 0.24	10.8 ± 0.5		5333 → 0
5600.1 ± 0.5	0.83 ± 0.14		5600 → 0

^a Relative to $I_{831}=1000$ for each decay. Can be converted to transitions per 100 decays by use of the factors 0.0278 for the $^{90}\text{Rb}^g$ decay assuming a ground-state β branch of 53%; and 0.0966 for the $^{90}\text{Rb}^m$ decay (no ground-state β decay is expected for the $3^- \rightarrow 0^+ ^{90}\text{Rb}^m$ β transition). The symbol w signifies that the relative intensity is less than 0.05.

^b Not placed in the level schemes. Intensity given as though in the $^{90}\text{Rb}^g$ decay.

^c Tentative placement. See discussion.

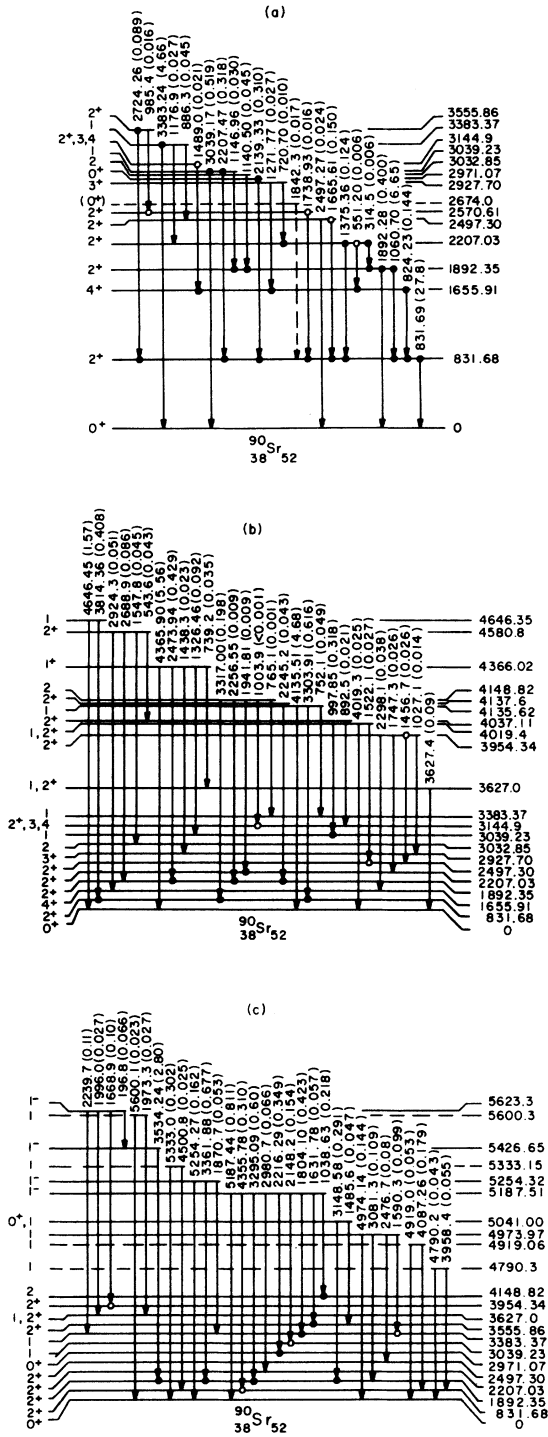


FIG. 6. Level scheme of ^{90}Sr populated in the decay of $^{90}\text{Rb}^s$. Coincidences are indicated by filled circles at the transition start and termination points (probable coincidences, by open circles). Intensities for the transitions are indicated per 100 decays. (a) levels to 3555 keV; (b) levels from 3627 to 4646 keV; (c) levels from 4790 to 5623 keV. Note that not all lower levels are shown in (b) and (c).

Figs. 6 and 7, respectively. The construction of these level schemes evolved from first constructing a composite level scheme and later splitting the composite into two decay schemes on the basis of γ -ray attributions. In this process, it was assumed that strong β feeding of the higher excited states in one decay precluded β feeding in the other decay, which is reasonable considering the spin differences involved in transitions from both the ground-state and isomer decays. Hence, the level schemes presented contain exclusive β

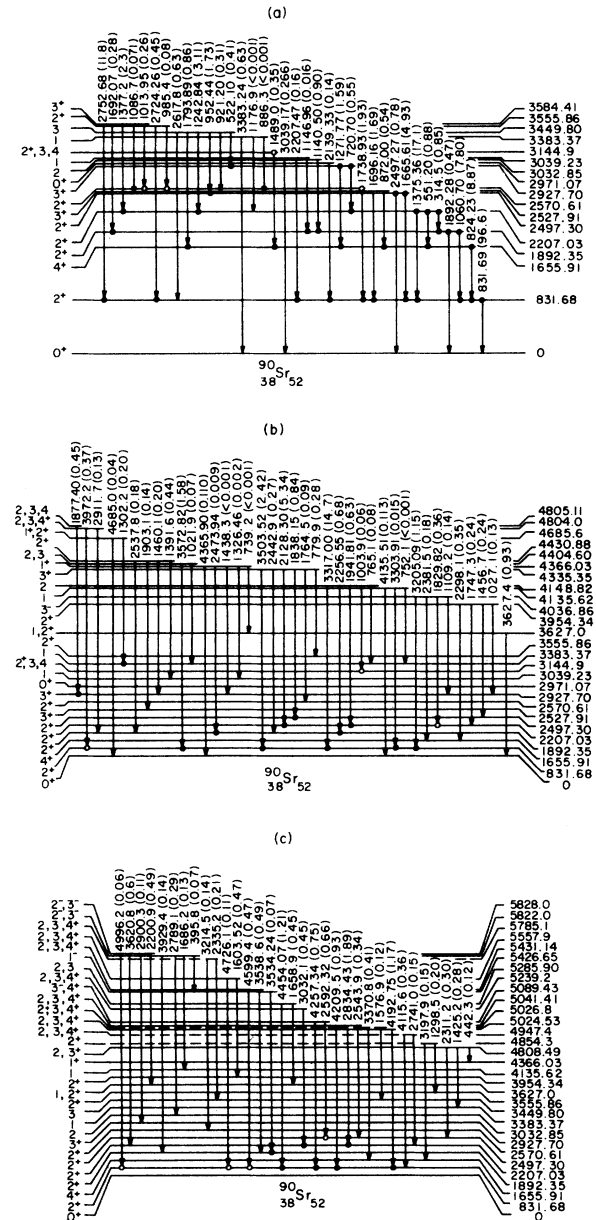


FIG. 7. Level scheme of ^{90}Sr populated in the decay of $^{90}\text{Rb}^m$. (a) levels to 3584 keV; (b) levels from 3627 to 4805 keV; (c) levels from 4808 to 5828 keV.

feeding to the higher levels. A level was considered definite only if three or more transitions, or definite coincidence information, could be included with the level. The dashed levels were established on the basis of fewer than three associated transitions in the absence of definite coincidence information. For the sake of brevity, virtually all the coincidence data are indicated on the level schemes, as explained in the caption to Fig. 6. It is notable that levels at 5041 and 4037 keV appear in both decays, at slightly different energies and with different depopulating transitions.

The level scheme presented in this work for the decay of $^{90}\text{Rb}^f$ consists of 33 excited states, 21 of which were not reported for the same decay in Ref. 13. These results reflect the relative ease in observing the ground-state decay transitions when analyzing ^{90}Rb decays as decay products of ^{90}Kr . For the isomer decay, however, the level scheme presented here contains 16 levels not reported in Ref. 13, and does not include five levels reported in the earlier work. The levels at 3316 and 4099 keV reported in Ref. 13 involve single transitions for which the reported coincidences are not reproduced in our studies; hence we have placed the transitions elsewhere. The 4893- and 5163-keV levels in Ref. 13 have single transitions that are not placed in this work because of the lack of definitive coincidence evidence. The 3008-keV level of Ref. 13 involves a single transition that was not observed in this work, probably because of the interference posed by the 1118-keV most intense transition in the decay of ^{90}Kr .

Intensity balances to all excited states were used to calculate the absolute β branchings and the $\log ft$ values shown in Table II. The $^{90}\text{Rb}^m$ ground-state branch was set equal to zero because it corresponds to a third-forbidden β decay. The $^{90}\text{Rb}^f$ ground-state branch was determined to be $53 \pm 5\%$. This determination replaces the previous value²⁰ of $37 \pm 5\%$, which was based on our earlier, less complete level schemes in which the attributions were not completely worked out as in the present schemes.

The most notable difference between the present β branchings and those of Huang *et al.*¹³ involves the 831-keV level fed from the $^{90}\text{Rb}^m$ decay. Our results indicate substantial β branching to this level in the $^{90}\text{Rb}^m$ decay, which is supported by the recent Q_β study of Decker *et al.*¹¹ In the latter work, γ -gated β spectra were obtained for five γ rays in the ^{90}Rb decay. The 831-keV gated spectrum did not exhibit the characteristic first-forbidden unique shape expected if this 2^+ level were fed only by 0^- $^{90}\text{Rb}^f$. Decker *et al.*¹¹ conclude that

the $^{90}\text{Rb}^m$ decay also feeds the 831-keV level but give no quantitative estimate. However, their estimate of $15 \pm 5\%$ ground-state branching for their combined $^{90}\text{Rb}^m$ and $^{90}\text{Rb}^f$ source and our absolute values for β branching give the result that their combined source had $29 \pm 10\%$ $^{90}\text{Rb}^f$ activity. With 2.5 times more $^{90}\text{Rb}^m$ than $^{90}\text{Rb}^f$ in their source, only about 30% of the β feeding of the 831-keV level would be from $^{90}\text{Rb}^f$, and hence the lack of a characteristic first-forbidden unique shape is understandable. Other differences between the decay schemes presented here and those reported in Ref. 13 are that the 1892-keV level is β fed in both decays here, and that no definite allowed β transitions (that is, $\log ft < 5.9$) are indicated to the 3584-, 4148-, and 4335-keV levels for the decay of $^{90}\text{Rb}^m$.

Spin-parity assignments have been made for the levels in Figs. 6 and 7 using the γ - γ angular correlation results in conjunction with the (t, p) results¹⁵ and β and γ branching information. The angular correlation results¹⁸ are summarized in Table III and provide a starting point for many of the assignments. In the assignment of spin-parity to the levels of ^{90}Sr , several assumptions are used in the interpretation of the angular correlation data. First, it is assumed that no transitions of significant intensity have multipole order L greater than 2. Next, it is assumed that mixed dipole/quadrupole transitions in which the quadrupole contribution to the total intensity is greater than about 10% are $M1/E2$ transitions, rather than $E1/M2$, and that these transitions therefore connect states of the same parity. Finally, spin 2 levels that display significant branching to the 0^+ ground state are assumed to have even parity. Combined with the angular correlation and (t, p) results, the rules of Raman and Gove²¹ were used to deduce level spin-parity assignments on the basis of the observed $\log ft$ values, and in association with the observed γ -ray transitions. These several approaches allowed many of the levels to be assigned unique spins, or at least the range of spins to be significantly limited. The 0^+ , 2971-keV level, searched for previously in Ref. 6, had an angular correlation that was quite distinctive.

There is disagreement with the (t, p) assignment,¹⁵ principally for the level at 2207 keV, for which a 2^+ assignment is made here, and which seems irrefutable from the angular correlation results (see the 1375-keV correlation in Fig. 5). Note, also, that the (t, p) results are not consistent with the other evidence in this work for the spin assignments of the 2527-, 3144-, 3584-, and 5187-keV levels, and it is questionable that the same levels are being seen in both studies.

TABLE II. β branching and $\log ft$ values for $^{90}\text{Rb}^{s,m}$ decays.

Level energy (keV)	Ground-state decay		Isomer decay	
	Percent branching	$\log ft^a$	Percent branching	$\log ft^b$
0.00	53 \pm 5	7.12 \pm 0.04 ^c	0 (assumed)	
831.68 \pm 0.04	18.2 \pm 2.1	7.32 \pm 0.05 ^c	16 \pm 4	7.63 \pm 0.10 ^c
1655.91 \pm 0.08	\sim 0		3.6 \pm 0.6	7.98 \pm 0.08 ^c
1892.35 \pm 0.05	1.93 \pm 0.24	7.89 \pm 0.06 ^c	4.3 \pm 0.6	7.83 \pm 0.06 ^c
2207.03 \pm 0.05	\sim 0		3.2 \pm 1.1	7.81 \pm 0.15 ^c
2497.30 \pm 0.07	\sim 0		1.53 \pm 0.22	8.00 \pm 0.06 ^c
2527.91 \pm 0.07			1.77 \pm 0.13	7.92 \pm 0.03 ^c
2570.61 \pm 0.09	\sim 0		1.36 \pm 0.12	8.03 \pm 0.04 ^c
2927.70 \pm 0.08	\sim 0		0.90 \pm 0.25	8.02 \pm 0.12 ^c
2971.07 \pm 0.18	\sim 0		\sim 0	
3032.85 \pm 0.07	\sim 0		0.62 \pm 0.19	8.14 \pm 0.14 ^c
3039.23 \pm 0.07	0.30 \pm 0.05	8.16 \pm 0.07 ^c	\sim 0	
3144.9 \pm 0.4	\sim 0		0.30 \pm 0.06	8.39 \pm 0.08 ^c
3383.37 \pm 0.09	4.0 \pm 0.4	6.84 \pm 0.05	\sim 0	
3449.80 \pm 0.06			6.7 \pm 0.3	6.87 \pm 0.03
3555.86 \pm 0.16	\sim 0		\sim 0	
3584.41 \pm 0.08			14.7 \pm 1.0	6.45 \pm 0.03
3627.0 \pm 0.3	\sim 0		\sim 0	
3954.34 \pm 0.19	\sim 0		0.48 \pm 0.22	7.70 \pm 0.20 ^c
4019.4 \pm 0.4	0.05 \pm 0.02	8.32 \pm 0.13 ^c		
4036.86 \pm 0.13			1.83 \pm 0.15	7.01 \pm 0.04
4037.11 \pm 0.09	0.30 \pm 0.04	7.55 \pm 0.06 ^c		
4135.62 \pm 0.10	5.3 \pm 0.6	6.22 \pm 0.05	\sim 0	
4137.6 \pm 0.9	0.04 \pm 0.03	8.3 \pm 0.3 ^c		
4148.82 \pm 0.09	\sim 0		16.1 \pm 0.7	6.03 \pm 0.03
4335.35 \pm 0.07			9.2 \pm 0.4	6.14 \pm 0.03
4366.03 \pm 0.11	6.1 \pm 0.6	5.98 \pm 0.05	\sim 0	
4404.60 \pm 0.18			1.65 \pm 0.12	6.83 \pm 0.04
4430.88 \pm 0.23			0.96 \pm 0.13	7.04 \pm 0.06
4580.8 \pm 0.3	0.23 \pm 0.04	7.22 \pm 0.08		
4646.35 \pm 0.14	1.98 \pm 0.21	6.22 \pm 0.05		
4685.6 \pm 0.3			0.23 \pm 0.06	7.44 \pm 0.10 ^c
4790.3 \pm 0.5	0.10 \pm 0.02	7.39 \pm 0.10		
4804.0 \pm 0.5			0.50 \pm 0.09	7.00 \pm 0.08
4805.11 \pm 0.22			0.45 \pm 0.05	7.04 \pm 0.05
4808.49 \pm 0.22			0.70 \pm 0.10	6.85 \pm 0.07
4854.3 \pm 0.4			0.35 \pm 0.07	7.10 \pm 0.09
4919.06 \pm 0.20	0.23 \pm 0.03	6.88 \pm 0.06		
4947.4 \pm 0.4			0.51 \pm 0.10	6.85 \pm 0.08
4973.97 \pm 0.17	0.43 \pm 0.07	6.56 \pm 0.07		
5024.53 \pm 0.24			1.17 \pm 0.11	6.41 \pm 0.05
5026.8 \pm 0.3			0.53 \pm 0.07	6.75 \pm 0.06
5041.00 \pm 0.13	0.34 \pm 0.04	6.58 \pm 0.06		
5041.41 \pm 0.12			3.16 \pm 0.19	5.96 \pm 0.04
5089.43 \pm 0.16			1.41 \pm 0.10	6.26 \pm 0.04
5187.51 \pm 0.06	3.0 \pm 0.3	5.46 \pm 0.05		
5239.2 \pm 0.5			0.44 \pm 0.07	6.59 \pm 0.07
5254.32 \pm 0.12	0.89 \pm 0.10	5.90 \pm 0.05		
5285.90 \pm 0.20			1.65 \pm 0.11	5.96 \pm 0.04
5333.15 \pm 0.24	0.33 \pm 0.04	6.24 \pm 0.06		
5426.65 \pm 0.13	2.7 \pm 0.3	5.18 \pm 0.06	\sim 0	
5431.14 \pm 0.25			0.96 \pm 0.11	6.00 \pm 0.06
5557.9 \pm 0.3			0.58 \pm 0.06	6.04 \pm 0.05
5600.3 \pm 0.5	0.05 \pm 0.01	6.65 \pm 0.11		
5623.3 \pm 0.3	0.31 \pm 0.08	5.81 \pm 0.12		

TABLE II. (Continued)

Level energy (keV)	Ground-state decay		Isomer decay	
	Percent branching	$\log ft^a$	Percent branching	$\log ft^b$
5785.1 \pm 0.8			0.35 \pm 0.10	5.88 \pm 0.13
5822.0 \pm 0.5			0.63 \pm 0.21	5.56 \pm 0.15
5828.0 \pm 0.4			1.26 \pm 0.24	5.25 \pm 0.09

^a Calculated using the proposed decay scheme and $Q_\beta = 6.55 \pm 0.06$ MeV.

^b Calculated using the proposed decay scheme and $Q_\beta = 6.66 \pm 0.06$ MeV.

^c $\log ft > 8.5$, so cannot exclude first-forbidden unique transition.

A final result to report is the equilibrium ratio of $^{90}\text{Rb}^m$ to $^{90}\text{Rb}^f$ activities, as originating from the decay of ^{90}Kr . Analysis of 22 transitions in the equilibrium spectrum yields an activity ratio of $(16 \pm 1\%)$, compared to the activity ratio derived from intensity balances in the decay of ^{90}Kr of $(15 \pm 1\%)$. These numbers compare well with the activity ratio deduced in the study of Mason and Johns.⁵

IV. DISCUSSION

One of the striking features of the level structure of ^{90}Sr that results from the interpretation of the results of the present work and other studies is that, despite the presence of a reasonably high spin value for $^{90}\text{Rb}^m$, the possibility of β decay followed by γ decay to high-spin states in ^{90}Sr is apparently not realized. The fact that

TABLE III. Correlation coefficients and spin assignments in ^{90}Sr .

Level (keV)	Cascade (keV)	A_2	A_4	Percent $L=2$	Spin of level
1655	824-831	0.12 \pm 0.05	0.04 \pm 0.06		4
1892	1060-831	-0.105 \pm 0.016	0.083 \pm 0.018	20 \pm 2	2 ⁺
2207	1375-831	-0.089 \pm 0.013	0.051 \pm 0.015	18 \pm 1	2 ⁺
2497	1665-831	0.23 \pm 0.03	0.02 \pm 0.03	0.5 \pm 0.5	2
2527	871-(824)-831	0.03 \pm 0.11	-0.15 \pm 0.11	99 \pm 1	(3 ⁺)
2570	1738-831	-0.17 \pm 0.07	0.11 \pm 0.08	28 $^{+11}_9$	2 ⁺
2927	1271-(824)-831	0.18 \pm 0.05	0.01 \pm 0.05	16 \pm 5 ^a or \leq 6	(4, 3 ⁺)
2971	2139-831	0.23 \pm 0.12	1.28 \pm 0.14		0
3032	1140-(1060)-831	0.31 \pm 0.13	0.11 \pm 0.16		2
3039	2207-831	-0.47 \pm 0.10	-0.01 \pm 0.11	5 $^{+8}_4$	1
3450	1793-(824)-831	-0.02 \pm 0.15	0.02 \pm 0.17		3
	1242-(1375)-831	0.01 \pm 0.04	-0.02 \pm 0.05	<6.6	
	952-(1665)-831	-0.10 \pm 0.09	0.16 \pm 0.11	65 to 100	
3555	2724-831	0.18 \pm 0.21	0.34 \pm 0.22	89 $^{+9}_{20}$	2 ⁺
3584	2752-831	0.24 \pm 0.03	-0.06 \pm 0.03	60 $^{+5}_{40}$	3 ⁺
4036	1829-(1375)-831	-0.24 \pm 0.22	-0.15 \pm 0.25		1, 2, 3
4037	997-(2207)-831	0.11 \pm 0.11	0.02 \pm 0.15	75 $^{+12}_{23}$ or 7 $^{+14}_6$	1, 2, 3 ^b
4148	2256-(1060)-831	0.08 \pm 0.21	0.21 \pm 0.24		1, 2, 3
4335	2128-(1375)-831	-0.07 \pm 0.03	0.05 \pm 0.04	95 to 100	(3, 1) ⁺
	1838-(1665)-831	0.29 \pm 0.14	0.18 \pm 0.16	21 to 69	
4366	2472-(1060)-831	-0.12 \pm 0.07	0.06 \pm 0.08	<2.7	1, 3

^a For spin 3. Other value for spin 4.

^b Percent $L=2$ values given for spin 2.

there are so few states observed with $J > 2$ for $E < 4$ MeV makes it difficult to account for the level structure in terms of expected shell-model configurations that give rise uniquely to high spins.

Comparing the present work with that of Flynn *et al.*¹⁵ suggests that an additional 0^+ level exists at 2674 keV. In fact, an unassigned transition at 1842.3 keV was observed in this work, and there is a very slight indication of a coincidence with the 831-keV transition at this energy. Hence, we have included a tentative level at 2674.0 keV, assigned as a 0^+ level. [The energy calibration for the (t, p) studies agrees well with our energies in this region; there is little ambiguity expected for the distinctive $L = 0$ two-nucleon transfer on the basis of energy alone.]

In addition to the general lack of high-spin states observed in this work, it is remarkable that we apparently do not observe a 3^- state at about 2.5 MeV expected on the basis of level systematics. The state at 2207 keV, reported as $3^-(4^+)$ in Ref. 15, is either not observed in this work, or is actually the 2^+ state we observe, and the 2527-keV state that we interpret as a 3^+ level could be the 3^- state expected. Our positive parity assignment is based on a nearly complete quadrupole character for the 871-keV γ ray, but it is possible that the transition character could be $M2$ rather than $E2$, and that the 871-keV γ ray connects levels through configurations that the $E1$ interaction cannot link. For example, if the 2527-keV state were 3^- and were strongly dominated by the configuration (relative to an ^{88}Sr core) $\nu(2d_{5/2}1h_{11/2})$, then no $E1$ deexcitation could occur and $M2$ deexcitations would occur to the $\nu(2d_{5/2}1g_{7/2})$ terms in the lower-lying 2^+ and 4^+ states.

Although our data indicate strongly that the 2207-keV level is 2^+ , we have evaluated the possible consequence of contributions from the unresolved 1377-keV transition to the 1375-831 cascade angular correlation. This evaluation was made to consider if the previous conclusion that the 2207-keV level is 2^+ could be modified to conform to the 3^- assignment favored in the (t, p) study.¹⁵ The contribution of the 1377-(1375)-831 γ -skip- γ cascade to the measured angular correlation was estimated in the extreme limit of a 1377($E2$)-1375($E1$)-831($E2$) cascade, representing a 3-3-2-0 spin sequence, and for the most extreme intensity ratio. (The 3584-keV level was also assigned as 3^- , or 4^+ , in Ref. 15.) This approach yields $A_2 = -0.076$ and $A_4 = +0.024$ for the nominal 1375-831 correlation, compared to the measured values of -0.089 ± 0.013 and $+0.051 \pm 0.015$, respectively. We conclude that, even considering

the most extreme interference in the 1375-831 angular correlation measurement from the 1377-keV transition, there is not adequate motive to change our original assignment of the 2207-keV level as 2^+ . Further measurements would be required to resolve the issue of the 2207-keV level spin assignment, with (t, p) studies possibly being the most definitive.

Of particular note in the two decay schemes presented is the absence of any clearly allowed β transitions to levels below 5 MeV. This situation impedes any speculation concerning simple configurations for levels involving neighboring shell-model states, because at such a high-excitation energy the levels are expected to have complex configurations. The suggestion by Ekström *et al.*⁴ that the large magnetic moment of $^{90}\text{Rb}^m$ can be accounted for by a dominant configuration of the seniority-3 state $\nu(2d_{5/2})_{3/2}^3$ would also serve to explain the relative similarity of the decay of $^{90}\text{Rb}^m$ with $^{90}\text{Rb}^f$ (in that no striking differences in the β strength functions are evident).

The level structure of ^{90}Sr appears to be characteristic of a spherical nucleus, at least in the excitation range less than about 3 MeV. This is to be expected, because the closed-shell nucleus ^{88}Sr is neighboring. The excitation progression of low-spin, positive-parity states up to about 3 MeV can be approximately accounted for by neutron excitations involving the positive-parity orbitals $2d_{5/2}$, $3s_{1/2}$, $2d_{3/2}$, and $1g_{7/2}$, in appropriate combination. Without more information to draw upon, for example, single-particle transfer reaction data, it is not instructive to attempt assignment of the levels observed. The development of facilities to study charged-particle reactions using radioactive targets could yield important configuration information from the (d, p) reaction on 50- d ^{88}Sr .

The results of this work present considerable new information on the levels in ^{90}Sr , but there is little to be seen in a presentation of the level systematics for even Sr nuclei until more is known about the general features of level schemes for $N > 52$. Despite the recent results reported on the level structure of ^{92}Sr (in which the 0^+ level systematics are displayed),²² and the newly reported information on the levels of ^{94}Sr and ^{96}Sr ,²³ and ^{98}Sr ,²⁴ it remains difficult to trace levels through the $\nu(2d_{5/2})$ subshell. This is, at least in part, due to the fluctuating spins of the decaying Rb nuclei (0^- and 3^- for ^{90}Rb , 0^- for ^{92}Rb , 3^- for ^{94}Rb , and apparently low for ^{96}Rb), which then give rise to level schemes that are not comparable. It remains a challenge to the capabilities of existing facilities to divulge more fully the structures of the very neutron-rich even-Sr nuclei (for ex-

ample, to locate the low-spin states in ^{94}Sr), needed for meaningful presentation of level systematics.

ACKNOWLEDGMENTS

One of the authors (C.L.D.) would like to acknowledge the support of the Alfred P. Sloan Foundation through its grant to Grinnell College. Because the

measurements reported here have spanned an unusually long time period, it is difficult to acknowledge the contributions of all individuals who have helped us in the experiments carried out at the TRISTAN facility in Ames. However, we would like to specifically mention the substantial efforts of J. R. McConnell, K. B. Nielsen, S. T. Hsue, and R. J. Hanson.

*Present address.

† Present address: II. Physikalisches Institut der J. Liebig Universität, 6300 Giessen, West Germany.

- ¹J. R. McConnell and W. L. Talbert, Jr., Nucl. Instrum. Methods 128, 227 (1975).
²C. L. Duke, W. L. Talbert, Jr., F. K. Wahn, J. K. Halbig, and K. Bonde Nielsen, Phys. Rev. C 19, 2322 (1979).
³D. C. Kocher, Nucl. Data Sheets 16, 55 (1975).
⁴C. Ekström, L. Robertsson, G. Wannberg, and J. Heinemeier, Phys. Scr. 19, 516 (1979).
⁵J. F. Mason and M. W. Johns, Can. J. Phys. 48, 2056 (1970).
⁶B. Singh and M. W. Johns, Can. J. Phys. 51, 865 (1973).
⁷G. H. Carlson, W. C. Schick, Jr., W. L. Talbert, Jr., and F. K. Wahn, Nucl. Phys. A125, 267 (1969).
⁸I. Amarel, R. Bernas, R. Foucher, J. Jastrzebski, A. Johnson, J. Teillac, and H. Gauvin, Phys. Lett. 24B, 402 (1967).
⁹A. H. Wapstra and K. Bos, At. Data Nucl. Data Tables 19, 177 (1979).
¹⁰F. K. Wahn and W. L. Talbert, Jr., Phys. Rev. C 18, 2328 (1978).
¹¹R. Decker, K. D. Wunsch, H. Wollnik, E. Koglin, G. Siegert, and G. Jung, Z. Phys. A 294, 35 (1980).
¹²M. I. Macias-Marques, A. Johnson, R. Foucher, and R. Henck, J. Phys. (Paris) 32, 237 (1971).

- ¹³H. Huang, B. P. Pathak, R. Iafigliola, L. Lessard, and J. K. P. Lee, Z. Phys. A 282, 285 (1977).
¹⁴D. C. Aumann and D. Weismann, J. Inorg. Nucl. Chem. 40, 1611 (1978).
¹⁵E. R. Flynn, O. Hansen, J. D. Sherman, N. Stein, and J. Sunier, Nucl. Phys. A264, 253 (1976).
¹⁶E. A. Henry, W. L. Talbert, Jr., and J. R. McConnell, Phys. Rev. C 7, 222 (1973).
¹⁷G. J. Basinger, W. C. Schick, Jr., and W. L. Talbert, Jr., Nucl. Instrum. Methods 124, 381 (1975).
¹⁸L. J. Alquist, Ph.D. thesis, Iowa State University, 1975 (unpublished).
¹⁹H. W. Taylor, B. Singh, F. S. Prato, and R. McPherson, Nucl. Data A9, 1 (1971).
²⁰F. K. Wahn, M. D. Glascock, W. L. Talbert, Jr., S. T. Hsue, and R. J. Hanson, Phys. Rev. C 13, 2492 (1976).
²¹S. Raman and N. B. Gove, Phys. Rev. C 7, 1995 (1973).
²²L. J. Alquist, H. Wollnik, G. Jung, B. Pfeiffer, P. Hungerford, S. M. Scott, and W. D. Hamilton, Nucl. Phys. A338, 1 (1980).
²³G. Jung, B. Pfeiffer, L. J. Alquist, H. Wollnik, P. Hungerford, S. M. Scott, and W. D. Hamilton, Phys. Rev. C 22, 252 (1980).
²⁴F. Schussler, J. A. Pinston, E. Monnard, A. Moussa, G. Jung, E. Koglin, B. Pfeiffer, R. V. F. Janssens, and J. Van Klinken, Nucl. Phys. A339, 415 (1980).